2025 IEEE World Haptics Conference (WHC)
Suwon Convention Center, Suwon, Korea
July 8 ~ 11, 2025

Modular, Multi-Layer e-Skin For Robotics Investigations and Applications

Alexis WM Devillard
Imperial College of Science, Technology & Medicine
London, UK
awd20@ic.ac.uk

Anirvan Dutta
Imperial College of Science, Technology & Medicine
London, UK
BMW Group, Munich, Germany
a.dutta22@imperial.ac.uk

Zhihuan Zhang
Imperial College of Science, Technology & Medicine
London, UK
zhihuazhang003@gmail.com

Xiaoxiao Cheng
Dept of Electrical & Electronic Engineering
University of Manchester
Manchester, UK
xiaoxiao.cheng@manchester.ac.uk

Mohsen Kaboli
BMW Group, Munich, Germany
Eindhoven University of Technology (TU/e),
Eindhoven, Netherlands
Mohsen.Kaboli@bmwgroup.com

Etienne Burdet
Imperial College of Science, Technology & Medicine
London, UK
eburdet@ic.ac.uk

***Abstract*—Like human skin, robotic electronic skin (e-skin) must protect the body from external threats and remain sensitive to the environment's characteristics while interacting with it. These conflicting requirements make e-skin design challenging. This work presents a modular, easy-to-replicate, and scalable bioinspired e-skin that uses layered silicone encapsulation with force-sensing arrays and accelerometers. This design enables control over the mechanical properties and sensor density, improving normal and shear force sensing and high-frequency vibration detection. The design allows us to seamlessly explore the mechanical properties of e-skin for sensing and adjust them for specific applications. We have characterized and systematically evaluated this e-skin using objects with controlled mechanical properties, demonstrating its ability to differentiate between texture, shape, and stiffness variations. Our e-skin design is versatile and can be adapted to various applications, including robotics, prosthetics, and virtual reality. The e-skin design files, code and documentation are available online, ensuring reproducibility and facilitating ongoing improvements.**

***Index Terms*—Electronic skin, tactile sensing, dexterous robotic manipulation, bioinspired functionalities, scalable fabrication**

I. Introduction

Designing effective haptic sensing systems is challenging due to the complexity of physical contact. The sense of touch can involve various sensations such as pressure, vibrations, temperature, chemical properties, etc. Capturing and interpreting these diverse signals requires advanced sensor technologies and processing algorithms [1]. In addition, sensors must be durable for repeated contact and sensitive enough to detect subtle changes. Compliance is also crucial to interact with objects with complex geometries and various soft and rough surfaces, requiring the sensing system to be flexible. Furthermore, integrating data from multiple sensors for high-fidelity touch sensing introduces added complexity, necessitating innovative electronic solutions and sophisticated algorithms for multi-modal data integration.

While extensive research has been devoted to developing artificial haptic sensors [2], much of this effort has focused on interaction with rigid objects. However, many real-world interactions involve soft and deformable objects, which present additional challenges, such as changes in shape, fragility, etc. Addressing these challenges requires sensors with specific mechanical and dynamic properties to effectively capture the force, vibrations, and other relevant information that arise during interaction [3].

Recent studies have explored bioinspired sensors replicating human skin's flexibility and sensory properties to address the challenges. However, their reliance on complex mechanisms [4], advanced materials [5], and intricate fabrication techniques [6] limits their accessibility and practicality for a systematic investigation of haptic interactions across diverse materials and sensing modalities. To complement the theoretical study of haptic interaction, more straightforward, adaptable, and robust artificial haptic sensors are required, facilitating the study of the mechanical properties of the sensor, optimal spatial and temporal resolution, and the importance of matching sensor properties to environmental conditions and tasks [7].

This work presents a multi-layered, modular, skin sensor based on simple, off-the-shelf and easy-to-fabricate components with certain functionalities inspired by biological skin (see Fig.1). The sensor platform is designed to investigate interactions with a wide range of rigid and soft materials, enabling the identification of interaction properties such as stiffness, texture, and dynamic response. Its modular layer design offers a practical sensing setup to study and model the role of the skin's mechanical properties on haptic sensing in controlled or real-world environments. All design files, code, and documentation are available online, ensuring repro-

This work was supported by the EC H2020 grants INTUITIVE (ITN 861166) and PH-CODING (FETOPEN 829186).

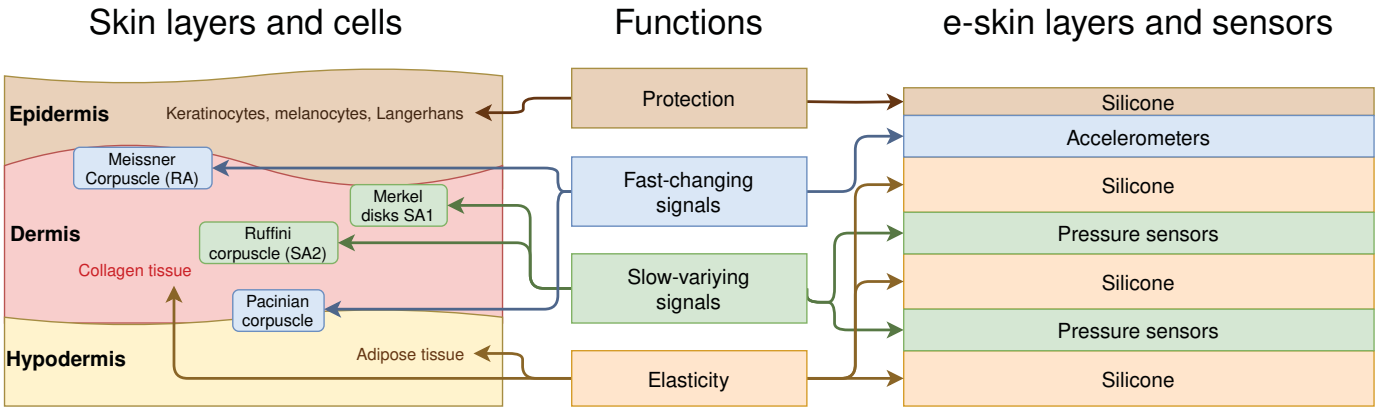

Fig. 1: **Human skin structure and bioinspired functions for the e-skin design. A diagram of a simplified model of the human skin with epidermis, dermis, and hypodermis layers is shown on the left. The middle column identifies the shared functions of the human skin and e-skin. A simplified diagram of the e-skin with the sensorized layers embedded in silicone is shown on the right.**

ducibility and facilitating ongoing improvements. A step-by-step tutorial is provided at https://aightech.github.io/e-skin/.

To illustrate the versatility of the system, we implemented and tested two sensing modalities: force and vibrations. The force-sensing module measures slow-changing normal and shear forces, while the vibration-sensing module captures high-frequency vibrations during interactions. This modular approach enabled rapid testing of sensor configurations and materials, providing insight into their effects on haptic perception. Using a robotic arm, we systematically evaluated sensor modalities, spatial and temporal resolution, and material types of the layers by interacting with diverse, curated and designed objects of varying stiffness and surface shapes, analyzing their impact on haptic perception.

II. Design and Fabrication

We developed an e-skin incorporating distributed load and vibration sensing capabilities to investigate the role of mechanical properties during haptic interactions. A key motivation for this work was the need for a simple and modular hardware platform to test a wide range of mechanical and sensing configurations, yet sophisticated enough to capture the complexity of haptic interaction and evaluate the impact of each combination of materials and sensors.

A. E-skin structure

To ensure modularity and scalability, the e-skin was designed using a layered approach inspired by the structure of human skin (Fig.1). Each layer is interchangeable and consists of specific materials and sensors tailored to control the mechanical properties and sensing capabilities, enabling adaptability to various applications. This modular design facilitates the replacement or modification of individual components, allowing the e-skin to be customized for different tasks or environments.

For the compliant layers, Smooth-On Ecoflex (Shore 00-31) and Dragonskin (Shore 30A) addition-cure silicone rubber were selected due to their flexibility, ease of handling and biocompatibility. The silicone layers were cast using 3D-printed moulds to achieve precise shapes and dimensions. Preliminary experiments were conducted to determine the optimal thickness and hardness of the silicone. It was observed that overly thick or compliant layers excessively filtered haptic signals, reducing sharpness and detail. Conversely, thin or overly rigid layers compromised the e-skin's ability to conform to complex surfaces. A balance was achieved, whereby the silicone provided sufficient compliance for effective deformation while maintaining enough rigidity for accurate signal capture. The experiment described in subsequent sections evaluates how variations in the different aspects of silicone layers influence the perception of object-skin interaction.

The final design of the e-skin comprises three sensorized layers embedded within compliant silicone, as shown in Fig.2.b. The outermost layer incorporates accelerometers to measure high-frequency vibrations, with functionality similar to rapidly adapting mechanoreceptors in human skin. Additionally, two layers of force-sensing resistors (FSRs) capture normal forces and deformations. While FSRs are inherently suited for detecting normal forces, they cannot directly sense shear forces. To address this issue, a compliant silicone interlayer is placed between the two FSR layers. Small shear displacements between these layers produce differential normal force, enabling shear force sensing. This design yields rich haptic sensing capabilities by capturing multi-modal data from the same contact area.

To address potential noise and interference in the FSR and accelerometer sensors, the e-skin leverages a multi-nodal configuration inspired by the redundancy of human mechanoreceptors. Each sensor layer consists of arrays of sensing units, providing overlapping coverage. This redundancy can improve the reliability of the tactile sensing, robustness to errors, and accuracy of the measurement. Furthermore, the layered structure of the e-skin introduces a degree of fault tolerance: the failure of one sensing unit does not compromise the system's overall functionality, ensuring robust performance

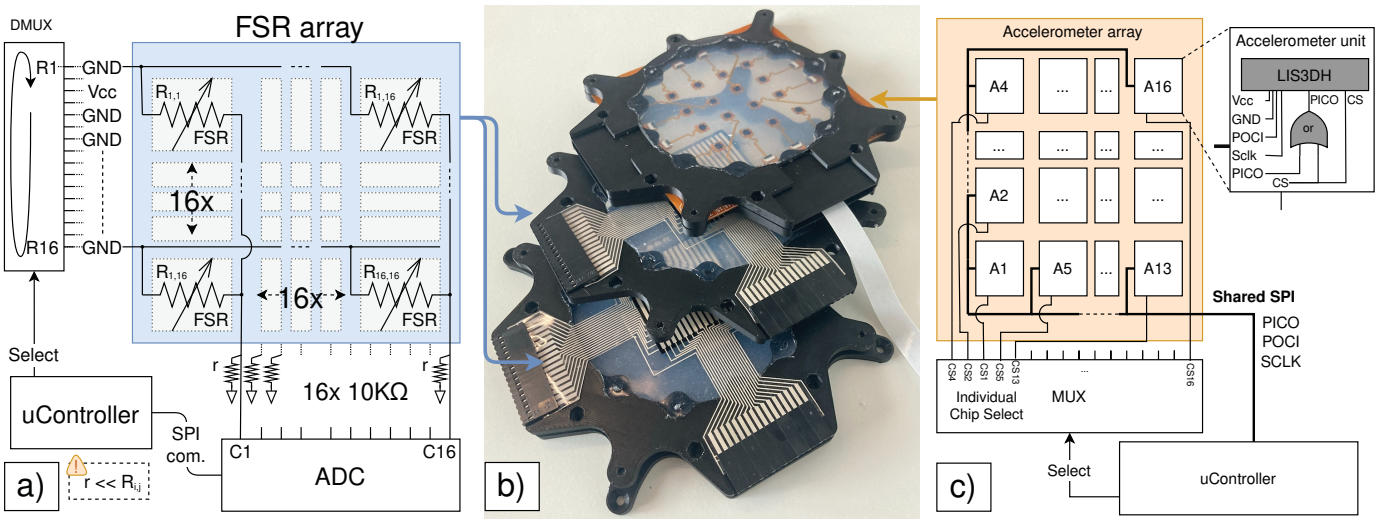

Fig. 2: **Our implementation of modular e-skin with the sensory layers and components displayed in (b). The FSR array electronic diagram is shown in (a), and the accelerometer array electronic diagram in (c).**

even under demanding conditions.

The accelerometer array layer was positioned near the top of the e-skin, just below a thin silicone layer, to minimize damping from affecting the high-frequency vibrations sensing. Accelerometers are ideal for this purpose, as they are highly sensitive to rapid changes in acceleration and can detect subtle vibrations. A 4x4 array of 3-axis LIS3DH accelerometers (spaced 15mm appart) was used to capture these vibrations. The LIS3DH sensors (costing around 1 USD per unit) are affordable while having a suitable performance for our application (3×3 mm^2, 0.98 mg/LSB, ±16g). They offer three analog inputs, allowing future integration of additional sensing modalities such as temperature or humidity sensors.

To measure static or slowly varying normal and shear forces, the e-skin includes two layers of FSR arrays. The resolution of the FSR arrays determines the e-skin's ability to capture fine details and subtle changes in the contact surface. We used 16×16 FSR arrays from Roxifsr with sensing cells of 2×2 mm^2 and a 1 mm pitch.

The implemented e-skin measures approximately 120 mm $\times$ 120 mm $\times$ 25 mm. While suitable for applications involving robotic palms or large manipulators, this dimension may pose challenges for robotic fingertips. Miniaturisation could be achieved by employing custom smaller FSR units, denser flexible PCBs, and thinner silicone encapsulation, which would enhance its applicability in finer robotic manipulation tasks.

B. Electronic design

The electronic design necessary to capture and process tactile signals from e-skin sensors is a critical yet often overlooked aspect in the literature. While reading the outputs from a small number of sensors can be achieved using bulky laboratory equipment, scaling up to a larger number of sensors introduces significant challenges. These include managing wiring complexity, ensuring adequate data transfer rates, minimizing power consumption, and handling the increased data processing demands. These factors are crucial when designing an acquisition system capable of supporting e-skins with larger sensing areas or higher sensor densities. In this section, we present the developed electronic design for efficiently capturing and processing tactile signals from each sensor layer of our e-skin.

1) Accelerometer array: Capturing high-frequency vibrations from multiple sensors requires fast data transfer to a processing unit. While most accelerometers support both I2C and SPI protocols, the two-wire protocol I2C introduces significant latency in high-frequency data acquisition. It supports only a limited number of identical sensors per bus. SPI is faster and better suited for this purpose but requires a dedicated chip select line for each sensor and its three shared data lines, resulting in N+3 wires for N sensors. To reduce the wiring complexity, a demultiplexer was used to select each accelerometer via a four-bit address bus, decreasing the required communication lines to six for 16 sensors. The array's electronic design is shown in Fig. 2c.

When devices share a common bus, a critical challenge is to ensure that only the selected device responds to the communication and that other devices do not interfere. In our case, the LIS3DH, like many other accelerometers, can operate in both SPI and I2C modes, with the SPI chip select pin also determining the protocol selection. When multiple accelerometers are connected, an unselected SPI device reverts to I2C mode, causing any package resembling an I2C communication to be interpreted by all unselected accelerometers, leading to bus conflicts. This issue is not documented in the LIS3DH datasheet and was discovered during the development of the e-skin. To address this issue, we used an OR gate for each accelerometer to pull up the input line, effectively disabling I2C mode for unselected accelerometers.

Finally, to prevent vibration absorption by the PCB, each accelerometer was mounted on a small 4×4 mm^2 platform

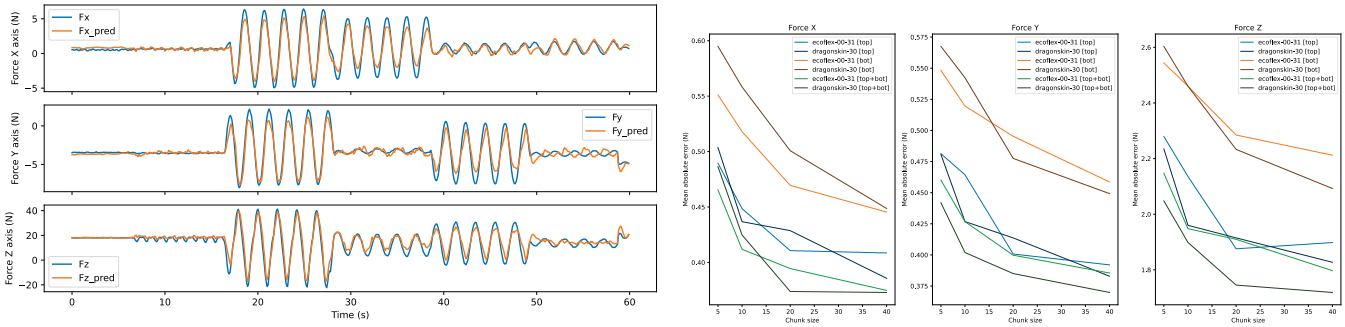

(a) Shear and Normal force estimation.

(b) Comparison of the force estimation accuracy.

Fig. 3: **Force estimation using the FSR arrays. (a) The plots show the shear and normal force estimation using the two FSR array layers with Ecoflex 00-31 silicone skin. (b) The plots compare the force estimation accuracy using different: skin types, number of FSR layers, and number of sample per sequence.**

linked to the main frame via a 3 mm wide, 0.2 mm thick flexible PCB bridge. This design allows the accelerometers to move freely, capturing subtle vibrations with minimal interference from the PCB structure.

2) FSR array: To avoid having to read each of the 256 sensors individually, the sensor array comprises 16 parallel conductive electrodes "rows" on one side of a resistive foam layer, while 16 perpendicular electrodes "columns" on the opposite side form a grid of intersecting nodes. Each intersection of a row and column functions as an independent sensing unit, resulting in a matrix of 256 discrete pressure-sensing points readable via only 32 wires. To scan the array efficiently, each row electrode is connected to a demultiplexer that sequentially applies voltage to each row, one at a time. On the column side, each of the 16 columns is connected to the ground through individual resistors, creating a network of voltage dividers with the resistive foam. When a force is applied to a sensing unit, the foam's resistance changes at that location, altering the voltage readout at the corresponding row and column. A parallel 16-channel Analog-to-Digital Converter (ADC) simultaneously measures the resulting voltages across all columns, effectively capturing a complete set of 256 reading points by activating each row. This process is illustrated in Fig.2.a. To prevent curent path into several combination of FSR cell, we ensure the resistors used to read the voltage at the output of the FSR array remain largely inferior to the FSR cells resistance values.

3) Data acquisition and processing: A Teensy 4.1 microcontroller was used to acquire and synchronize data. The 600 MHz clock speed makes it possible to read the 16 accelerometer 3-axis value and the 2×256 FSR values at a rate of 700 Hz. Additionally, Teensy 4.1 supports high-speed USB (480 Mbit/s), making it possible to stream the data to a computer in real-time.

III. Experiment

To evaluate and collect data from the e-skin, it was mounted on the end-effector of a Kinova robotic arm (Fig. 4a). A 6-axis force/torque sensor (ATI Nano 17) was attached between the e-skin and the robotic arm to provide a ground truth of the loads applied to the e-skin. The robotic arm was programmed to move the e-skin in predefined trajectories to interact with tested objects (Fig. 4b). A single computer controlled the robotic arm and collected the data from the e-skin and the force/torque sensor to ensure data synchronization.

A. Experimental objects

To evaluate the e-skin's performance systematically, we designed a set of "wave objects" with controlled mechanical properties (see Fig. 4c). These objects were used to generate haptic data under different controlled conditions, providing insight into the e-skin's ability to differentiate between texture, shape, and stiffness variations, thus serving as a foundational dataset.

1) Wave objects: The wave objects are characterized by three primary parameters: amplitude, spatial frequency, and stiffness. To create the surface of the wave objects, we applied a bandpass filter to a white noise image centred around one of three spatial frequencies $\{10/\text{m}, 30/\text{m}, 50/\text{m}\}$ with a bandwidth of 5/m. Using filtered noise allowed us to compensate for the limited number of discrete variations available for each parameter, introducing subtle deviations and a wider variety of surface characteristics. This method provided a more diverse representation of partially overlapping spatial frequencies, which helped incorporate intermediate features and reduce the rigidity of parameter categorization. The amplitude of the waves was controlled by scaling the filtered and normalized surface at three levels $\{5,10,20\}$mm. Each generated surface was mirrored and 3D printed to create molds for fabricating the object in silicone. The stiffness of the wave objects varied based on the materials used {Ecoflex 00-10, Ecoflex 00-50, rigid PLA}, which have specific Shore hardness values.

B. Interaction Protocol

To create a rich dataset of mechanical interactions, we used movements combining translation and rotational motion of the e-skin on the object's surface. The robotic arm was controlled

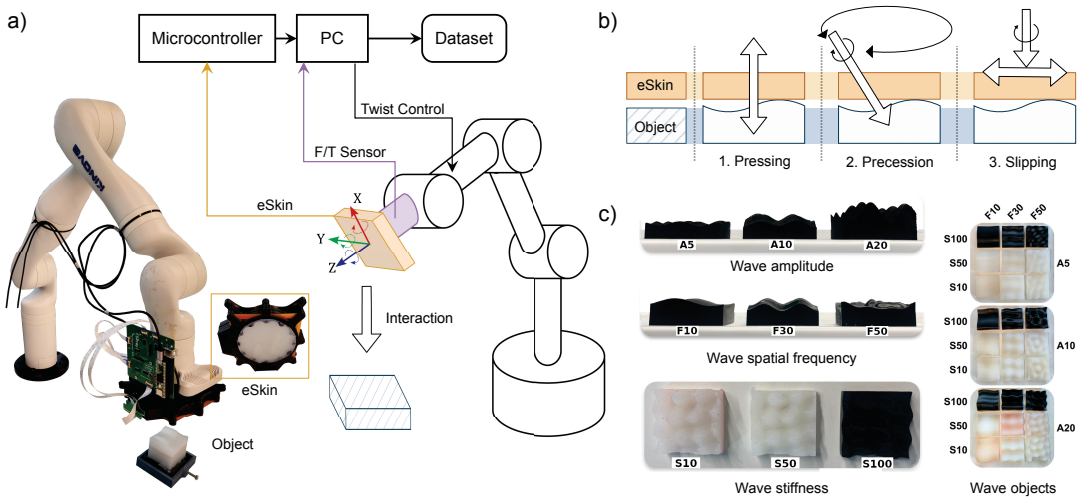

Fig. 4: **Experimental setup to evaluate the e-skin. The e-skin is mounted on the end-effector of a Kinova robotic arm (a), which is programmed to move the e-skin on predefined trajectories (b) in order to interact with tested objects (c).**

using a twist controller that regulated the end-effector's linear and angular velocities as illustrated in Fig. 4b:

- Pressing: In the pressing interaction, the robotic arm moves along the z-axis with

$$z(t) = A\cos\left(2\pi\omega t + \pi\right) \tag{1}$$

  This motion enables precise measurement of the deformation and depth properties of rigid and compliant materials. By varying the amplitude and frequency of the sinusoidal motion, we could simulate different force profiles and characterize the response of the e-skin under various pressure conditions.
- Precession: In this protocol, the end effector and electronic skin rotate around the x- and y-axes, allowing interaction with different areas of the object's surface. This method is especially effective for evaluating complex geometrical features, such as concave or convex regions, by providing haptic feedback from multiple angles of interaction, represented as roll (α) and pitch (β) angles:

$$\alpha(t) = A\sin\left(2\pi\omega t + \frac{\pi}{2}\right), \quad \beta(t) = A\sin\left(2\pi\omega t\right) \tag{2}$$

- Slipping: During the slipping interaction, the e-skin executes a controlled sequence of translational and rotational motions to simulate natural human texture exploration. It first slides linearly along the X and then Y axes, followed by a circular twisting motion around the Z axis. This interaction allows the e-skin to gather detailed data on surface roughness, texture, and friction, providing a more comprehensive dataset for analyzing the physical surface properties of various materials. The interaction is combining translation xy and rotation θ:

$$xy(t) = A\sin\left(2\pi\omega t\right), \quad \theta(t) = A\sin\left(2\pi\omega t\right) \tag{3}$$

where the amplitude parameters A and the frequency parameters ω are specific to each of the above movement types. We performed an initial experimental evaluation to determine the range of the parameters, taking into account the robot controller frequency and sensor saturation. Within this range, 16 values were uniformly sampled to perform the interactive actions using the robotic setup and the objects. Combining these actions and parameter variations resulted in a rich dataset well-suited for evaluating the e-skin's performance across a broad spectrum of interaction scenarios. The parameters for each trial are detailed in Table I.

Trials	Pressing		Precession		Slipping		
	A_{press} (mm)	ω (Hz)	A_{angle}	ω (Hz)	A_{slide} (mm)	A_θ (°)	$\omega\,(Hz)$
1	2	0.2	3°	0.2	2	3°	0.2
2	2	0.4	3°	0.4	2	3°	0.4
3	2	0.6	3°	0.6	2	3°	0.6
4	2	0.8	3°	0.8	2	3°	0.8
5	4	0.2	4°	0.2	4	4°	0.2
6	4	0.4	4°	0.4	4	4°	0.4
7	4	0.6	4°	0.6	4	4°	0.6
8	4	0.8	4°	0.8	4	4°	0.8
9	6	0.2	5°	0.2	6	5°	0.2
10	6	0.4	5°	0.4	6	5°	0.4
11	6	0.6	5°	0.6	6	5°	0.6
12	6	0.8	5°	0.8	6	5°	0.8
13	6	0.2	6°	0.2	8	6°	0.2
14	8	0.4	6°	0.4	8	6°	0.4
15	8	0.6	6°	0.6	8	6°	0.6
16	8	0.8	6°	0.8	8	6°	0.8

TABLE I: **Action parameters for the experiment's 16 trials.**

C. Data collection and preprocessing

Data collection started with a 5 s calibration phase, during which the robotic arm and e-skin remained stationary in contact with the object to collect baseline data for noise filtering and sensor correction. For each object, 16 trials were performed across the three interaction protocols, with key parameters varied to ensure diversity. Force and torque data were captured using the ATI Nano 17 sensor at 1 kHz, which was downsampled to 100 Hz and synchronized with the end-effector pose data using a mean filter to reduce Gaussian-like noise. The e-skin system comprised two 16×16 FSR layers and a 4×4×3 accelerometer layer recorded at a sampling frequency of 700 Hz. After recording, the data for

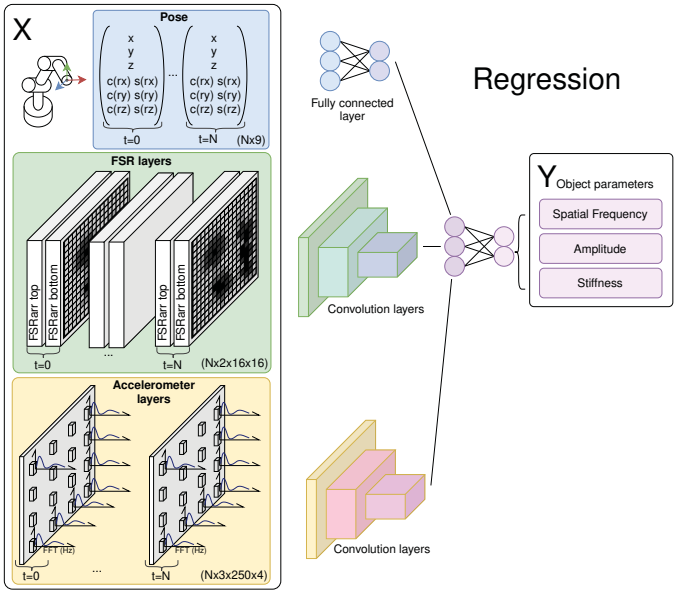

Fig. 5: **Structure of the neural network used to regress the tactile data from the FSR and accelerometer to the spatial frequency, amplitude, and stiffness of each object. The input samples consist of chunks of NN sequential data points, including the robot pose, data from two layers of FSR arrays, and the accelerometer data. The network is trained to predict the spatial frequency, amplitude, and stiffness of the objects based on the pressure and accelerometer data.**

each modality were normalized to $[-1, 1]$ using their respective minimum and maximum values in all trials to analyze the response of the e-skin in diverse interaction scenarios.

IV. Results

We evaluated our e-skin implementation by analyzing how various skin types, sensor layers, and sampling rates affect force and object parameter estimation.

A. Normal and shear force estimation

We evaluated the e-skin's ability to estimate normal and shear forces. Accurate shear force estimation is crucial for haptic sensing, enabling robots to detect lateral forces, assess friction, and detect slip during grasping, enhancing object manipulation and adaptability in dynamic environments. While FSRs were expected to capture normal forces effectively, shear force estimation was not inherently guaranteed and thus required validation. This first evaluation focused solely on the FSR array layers, excluding accelerometer data.

To capture the spatial and temporal dynamics of the FSR arrays, we employed a CNN-LSTM architecture [8], [9]. CNN extracted spatial features, while LSTM modeled temporal dependencies. Given the relatively slow variations in normal and shear forces, we downsampled the e-skin and ground-truth F/T data to 20 Hz, reducing the sequence length and sensor noise. A sliding window approach was adopted; shorter windows produced outputs more frequently, while longer windows considered more data to improve estimation accuracy. An ablation study was conducted using the same model architecture, examining the following factors to determine their impact on force estimation accuracy:

- Skin type: Ecoflex 00-31 or DragonSkin 30.
- Number of FSR layers: Top only, Bottom only, or both Top + Bottom layers.
- Number of samples per sequence: 5, 10, 20 or 40 samples.

Fig. 3a illustrates the shear and normal force estimations using the two FSR array layers with an Ecoflex 00-31 silicone skin of an exemplary observation. Fig. 3b and Table II present the estimation accuracy for different design parameters, highlighting key findings on e-skin's force estimation. For clarity, we also presented the results in Table II.

Axis	Layers	Skin type	Normalized mean error (N)				Mean error (N)			
			Number samples				Number samples			
			5	10	20	40	5	10	20	40
X	Top	Ecoflex 00-31	0.035	0.032	0.029	0.029	0.489	0.448	0.410	0.408
		DragonSkin 30	0.036	0.031	0.030	0.027	0.504	0.437	0.429	0.386
	Bot	Ecoflex 00-31	0.040	0.037	0.034	0.032	0.551	0.518	0.469	0.445
		DragonSkin 30	0.042	0.040	0.035	0.032	0.595	0.558	0.501	0.449
	Top+Bot	Ecoflex 00-31	0.033	0.030	0.028	0.027	0.465	0.412	0.394	0.375
		DragonSkin 30	0.034	0.030	0.026	0.026	0.486	0.425	0.374	0.373
Y	Top	Ecoflex 00-31	0.028	0.027	0.023	0.023	0.481	0.464	0.401	0.392
		DragonSkin 30	0.035	0.031	0.030	0.028	0.481	0.427	0.414	0.383
	Bot	Ecoflex 00-31	0.032	0.030	0.029	0.027	0.548	0.520	0.495	0.459
		DragonSkin 30	0.041	0.039	0.035	0.033	0.568	0.542	0.478	0.449
	Top+Bot	Ecoflex 00-31	0.027	0.025	0.023	0.023	0.460	0.427	0.400	0.385
		DragonSkin 30	0.032	0.029	0.028	0.027	0.442	0.402	0.385	0.370
Z	Top	Ecoflex 00-31	0.030	0.028	0.024	0.025	2.280	2.136	1.876	1.898
		DragonSkin 30	0.028	0.024	0.024	0.023	2.235	1.960	1.915	1.827
	Bot	Ecoflex 00-31	0.033	0.032	0.030	0.029	2.544	2.460	2.285	2.212
		DragonSkin 30	0.032	0.031	0.028	0.026	2.604	2.460	2.233	2.092
	Top+Bot	Ecoflex 00-31	0.028	0.025	0.025	0.023	2.147	1.948	1.910	1.797
		DragonSkin 30	0.025	0.024	0.022	0.021	2.048	1.899	1.745	1.719

TABLE II: **Force estimation accuracy for different skin types, number of FSR layers, and number of samples per sequence.**

The results show that Ecoflex 00-31 consistently surpassed DragonSkin 30 in accuracy. The two-layer FSR structure was designed primarily to capture shear forces through differential deformation between layers. While there was no significant difference in normal and shear force estimation, using the data of the two FSR layers (Top + Bottom) provided the most accurate force estimations, demonstrating the advantage of multi-layer data integration in capturing complex forces like shear from lateral movement. Furthermore, increasing samples per sequence improved accuracy, with 40 samples yielding optimal results, highlighting the role of temporal resolution in force estimation reliability. The model achieved a mean difference of about 1.7 N for normal and 0.4 N for shear forces. This difference is due to the different ranges of forces encountered on each axis. Normalization to the range [0,1] on each axis resulted in a mean error of 2% for normal and 3% for shear forces, showing the e-skin's effectiveness in quantifying forces in haptic interactions.

B. Wave object parameter estimation

A potential strength of our e-skin implementation is its multi-modal sensing capabilities, utilizing FSR for high-resolution force and static observation and accelerometers for detecting dynamic interactions and vibrations. We investigated the role of each modality and variations in e-skin mechanical properties for object recognition. To leverage these signals, we designed a multi-head, multi-modal network (see Fig. 5) where FSR and accelerometer data are processed separately

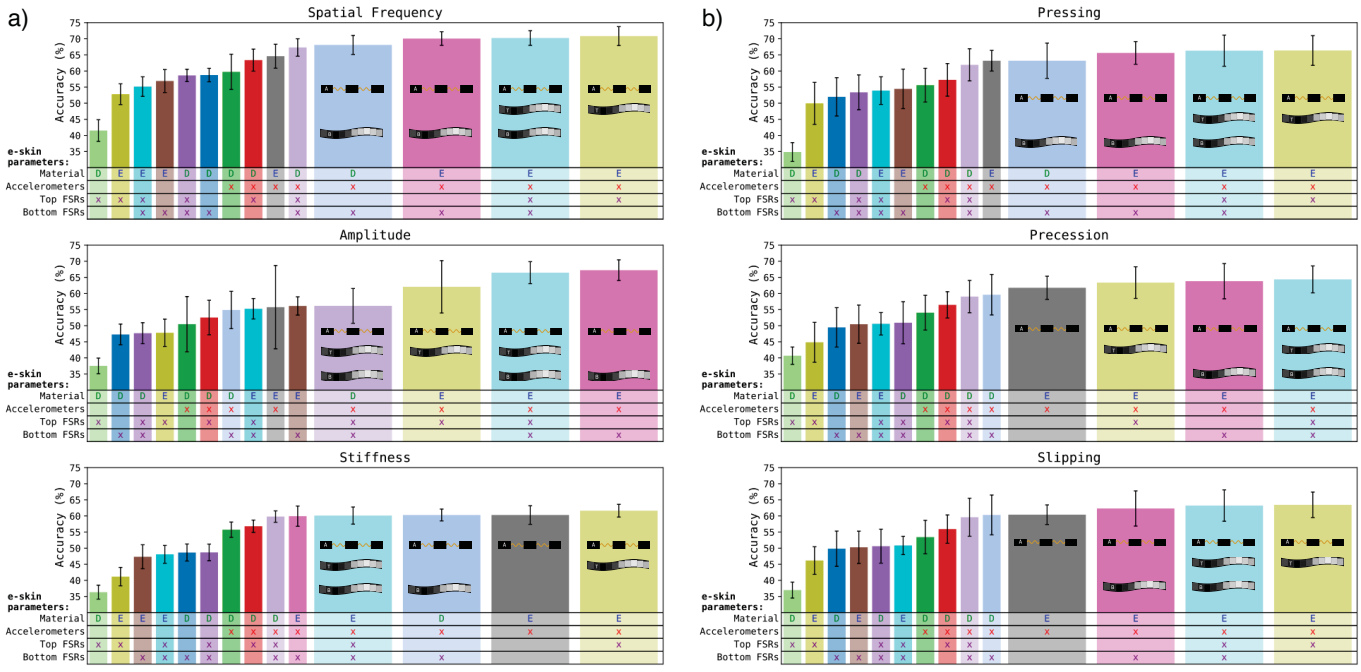

Fig. 6: **Classification results for all combinations of sensor configurations, material types, actions, and dimensions. The figure displays the ranking of all e-skin configurations based on the mean accuracy for a given dimension (spatial frequency, amplitude, stiffness) (a) and a given action (pressing, precession, slipping) (b).**

through 3D convolutional layers, extracting spatial and temporal features. The end-effector's position and orientation are encoded via a fully connected network (FCN), and all features are concatenated and passed through FC layers to predict object properties—spatial frequency, amplitude, and stiffness. A significant challenge in multi-modal integration is the differing temporal characteristics: FSR data is slow-varying, while accelerometers capture rapid fluctuations. We transformed accelerometer data into the spectral domain using short-time Fourier transforms to preserve dynamic information, aligning it with FSR data segments. This approach maintained high-frequency details while ensuring compatibility across modalities. We systematically analyzed how different FSR and accelerometer combinations impact objects' parameters estimation through an ablation study, evaluating the following factors:

- Skin type: Ecoflex 00-31 or DragonSkin 30.
- Number of FSR layers: None, Top only, Bottom only, or both Top + Bottom layers.
- Number of accelerometer layers: With or without accelerometer layers.
- Number of samples per sequence: 5, 10, or 20 samples.

This comprehensive evaluation enabled us to identify the optimal combination of sensor modalities and configurations for accurately predicting object properties, thereby maximizing the potential of the e-skin's multi-modal design. The results, illustrated in Fig. 6, offer a detailed analysis of how various sensor configurations and types of actions influence prediction accuracy for spatial frequency, amplitude, and stiffness. The regression model was trained to output a prediction of the central spatial frequency, amplitude, and stiffness of the object. We observed that the number of samples per sequence (5, 10, or 20) had a negligible effect on prediction accuracy and ranking. Therefore, the results presented in Fig. 6 reflect the average performance across these sample configurations.

Discussion

This study introduced an e-skin with layered silicone encapsulation, integrated FSR arrays, and accelerometer arrays. The layered silicone encapsulation enhances compliance and mechanical robustness, allowing for reliable interactions with various surfaces while maintaining durability. The eskin was used to record more than 1000 1-minute-long trials, demonstrating its robustness and reliability in continuous use. The system's implementation balances high temporal resolution (700 Hz for accelerometer layers) and spatial resolution (32 units/cm² for the FSR arrays), enabling it to capture static forces and dynamic interactions like vibrations. These features outperform many existing systems that either lack multi-modal integration or are limited in scalability and modular adaptability, as analyzed in Table III. A key advantage of our e-skin design is its ability to directly measure normal and shear forces directly, eliminating the need for external sensors and enabling cost-effective, integrated haptic sensing.

The use of e-skin in industrial applications is often limited by wiring complexity, as increasing the number of sensors typically leads to excessive cabling, making integration cumbersome and preventing the system from scaling properly. To address this, we focused on efficient multiplexing and

Implementation name	Robustness	Flexibility	Multimodality	Multi nodal	Spatial resolution	Temporal resolution	Modularity	Scalability	Ease of fabrication
Human skin	• Immune defence • Self-healing	Highly flexible	• Normal/shear force • Vibration • Temperature	✓	241 u./cm^2 on fingertips	400 Hz	N/A	N/A	N/A
Organic transistors [10]	Sensitive, limited durability	Highly flexible	Normal force	×	0.2u./cm^2	1KHz	No details	No details	Thin-film fabrication
Piezoelectric nanowire [6]	Stable under continuous use	Highly flexible	Vital signs	×	1u./cm^2	2Hz	No details	Self-powered	Nanopore fabrication
Polymer-waveguide [5]	Robust to bending	Thin-film	Normal force	✓	• 40u./cm^2 • 3x7 array	16Hz	No details	No details	Polymer waveguide
Large-Area sensor [11]	Robust to deformation	Highly flexible	Normal force	✓	• 16u./cm^2 • 32x32 array	No details	No details	• Maybe large-area • Electronic not detailed	Organic nano fabrication
FSR array [12]	• Plastic socket	• Rigid	Normal force	✓	• 1u./cm^2 • 32 FSR grid	20Hz	Interchangeable	No details	3D printing
Capacitive array [13]	• Silicone encapsulation	• Flexible • Stretchable	Normal force	✓	• 4u./cm^2 • 8x8 array	80Hz	Customisable Size	LCR circuitry maybe difficult to scale	Direct filament casting
BioTac [4]	Limited durability	Rigid finger	• Normal/shear force • Vibration • Temperature	×	N/A	100Hz	Self-contained module	Complex multi-layers	Precision fabrication
GelSlim [14]	Limited durability	Rigid sensorised layers	• Normal/shear force	✓	High-resolution optical sensing	30Hz	No details	High computational complexity	Precision fabrication
DIGIT [15]	Abrasion-resistant	Rigid sensorised layers	• Normal/shear force	✓	High-resolution optical sensing	60Hz	No details	High computational complexity	Precision fabrication
ReSkin [16]	• Durable • Reusable coating	Rigid sensorised layers	• Normal/shear force	✓	2.5 u./cm^2	400Hz	Interchangeable	Highly scalable	Simplified fabrication
Our e-skin	Silicone encapsulation	Flexible	• Normal/shear force • Vibration	✓	• 32 u./cm^2 • 2x 16x16 FSR • 4x4 accelero.	700Hz	Interchangeable sensor layers	Highly scalable using modular multiplexing	• 3D printing • Silicone moulding

TABLE III: **Comparison of tactile sensor and e-skin features across different implementations.**

sequential reading to minimize the number of wires per unit. The two FSR layers are interfaced using only seven wires for a total of 512 sensing units. The exact mechanism can be daisy-chained, enabling expansion where the required wires follow a scalable pattern of 5+N wires for N$\times$256 FSR sensing units. A similar approach was used for the accelerometer array, significantly reducing wiring overhead. Since each sensor consumes less than 15 µA of power, scaling the system remains feasible without significant increases in power consumption.

The modular design of the e-skin allowed us to evaluate different skin types rapidly. Our results demonstrate that the Shore hardness of the silicone layer significantly affects haptic sensing. In particular, using a softer layer (Ecoflex 00-31) improved force and object property estimation, likely due to better compliance and damping, enhancing signal transmission to the FSR arrays. The integration of high-frequency accelerometer data is critical in capturing subtle dynamic interactions, mirroring the principles of multi-sensory integration found in human skin. This was demonstrated from our experiments, as multi-modal haptic sensing improved the ability to capture fine-grained mechanical properties such as spatial frequency, amplitude, and stiffness of the wave object dataset.

A notable limitation of our current implementation is it's overall size and rigidness, which is not optimal and might not be suitable for all applications. However, the modular design allows for easy scaling and adaptation to various frame size and material configurations. Similarly, the scale of the objects used in our experiments was limited to surface spatial frequencies way below the spatial resolution of the e-skin, ensuring no aliasing effects. This setup could later be tested with smaller and sharper objects to evaluate the possibility of leveraging the e-skin's multi-modal sensing capabilities for more complex object properties.

In the future, we would like to explore more granular control over silicone stiffness to understand its role in haptic perception better. Additionally, incorporating ridges/structures in silicone layers (as inspired by the human fingertip skin) will also be interesting to amplify vibrations and further force transmission. Understanding the mechanical properties of e-skin is essential for improving robotic perception and manipulation, as well as transparent human-robot interactions. In general, the scalability and modularity of our e-skin design facilitate the integration of additional sensing modalities and functionalities, making it adaptable for diverse applications. We are currently working on the development of custom FSRs with flexible PCBs to offer greater design freedom, making these sensors adaptable to large areas and curved surfaces while maintaining accessibility and practicality for diverse applications.

CONCLUSION

We have developed a modular e-skin concept based on a layered silicone encapsulation and various sensory layers, demonstrated by an implementation with integrated FSR arrays and accelerometer arrays. Evaluations with controlled robot–object interactions showed accurate estimation of normal and shear forces and identification of object surface parameters. The design's modularity allowed the testing of different silicone materials, sensor arrangements, and layer configurations systematically.

The presented hardware and open documentation provide a reproducible approach to investigating haptic sensing mechanisms. The layout, electronics, and fabrication pipeline enable straightforward scaling to larger sensing areas, higher sensor densities or other sensing modalities. By combining modularity, compliance, and multi-modal sensing capabilities, our "hardware model" of the e-skin provides a suitable platform

for a large range of haptic sensing applications, from prosthetics to robotics.

REFERENCES

[1] S. Luo, J. Bimbo, *et al.*, "Robotic tactile perception of object properties: A review," *Mechatronics*, vol. 48, pp. 54–67, 2017.

[2] M. Meribout, N. A. Takele, *et al.*, "Tactile sensors: A review," *Measurement*, p. 115332, 2024.

[3] J. Hughes, L. Scimeca, *et al.*, "Online morphological adaptation for tactile sensing augmentation," *Frontiers in Robotics and AI*, vol. 8, p. 665030, 2021.

[4] J. A. Fishel and G. E. Loeb, "Sensing tactile microvibrations with the biotac—comparison with human sensitivity," in *IEEE RAS & EMBS Int. Conf. on Biomedical Robotics and Biomechatronics (BioRob)*, 2012, pp. 1122–1127.

[5] S. Yun, S. Park, *et al.*, "Polymer-waveguide-based flexible tactile sensor array for dynamic response," *Advanced Materials (Deerfield Beach, Fla.)*, vol. 26, no. 26, pp. 4474–4480, 2014.

[6] X. Chen, J. Shao, *et al.*, "Self-powered flexible pressure sensors with vertically well-aligned piezoelectric nanowire arrays for monitoring vital signs," *Journal of Materials Chemistry C*, vol. 3, no. 45, pp. 11 806–11 814, 2015.

[7] L. Costi, P. Maiolino, and F. Iida, "How the environment shapes tactile sensing: Understanding the relationship between tactile filters and surrounding environment," *Frontiers in Robotics and AI*, vol. 9, p. 930405, 2022.

[8] S. Hochreiter and J. Schmidhuber, "Long Short-Term Memory," *Neural Computation*, vol. 9, no. 8, pp. 1735–1780, 1997.

[9] J. Donahue, L. Anne Hendricks, *et al.*, "Long-term recurrent convolutional networks for visual recognition and description," in *Proc. IEEE Conf. on Computer Vision and Pattern Recognition*, 2015, pp. 2625–2634.

[10] J. Kim, T. Nga Ng, and W. Soo Kim, "Highly sensitive tactile sensors integrated with organic transistors," *Applied Physics Letters*, vol. 101, no. 10, p. 103308, Sept. 2012.

[11] T. Someya, T. Sekitani, *et al.*, "A large-area, flexible pressure sensor matrix with organic field-effect transistors for artificial skin applications," *Proceedings of the National Academy of Sciences*, vol. 101, no. 27, pp. 9966–9970, July 2004.

[12] N. Li, D. Yang, *et al.*, "Combined Use of FSR Sensor Array and SVM Classifier for Finger Motion Recognition Based on Pressure Distribution Map," *Journal of Bionic Engineering*, vol. 9, no. 1, pp. 39–47, Mar. 2012.

[13] B. Li, Y. Gao, *et al.*, "Soft capacitive tactile sensing arrays fabricated via direct filament casting," *Smart Materials and Structures*, vol. 25, no. 7, p. 075009, May 2016.

[14] W. Yuan, S. Dong, and E. H. Adelson, "Gelsight: High-resolution robot tactile sensors for estimating geometry and force," *Sensors*, vol. 17, no. 12, p. 2762, 2017.

[15] M. Lambeta, P. W. Chou, *et al.*, "DIGIT: A Novel Design for a Low-Cost Compact High-Resolution Tactile Sensor With Application to In-Hand Manipulation," *IEEE Robotics and Automation Letters*, vol. 5, no. 3, pp. 3838–3845, July 2020.

[16] R. Bhirangi, T. Hellebrekers, *et al.*, "ReSkin: Versatile, replaceable, lasting tactile skins," in *Proc Conference on Robot Learning*, June 2021.